35th Annual International Conference of the IEEE EMBS
Osaka, Japan, 3 - 7 July, 2013

Measurement of Radioactivity Concentration in Blood by Using Newly Developed ToT LuAG-APD Based Small Animal PET Tomograph

Azhar H. Malik[1], Kenji Shimazoe[2], and Hiroyuki Takahashi[3]

***Abstract*— In order to obtain plasma time activity curve (PTAC), input function for almost all quantitative PET studies, patient blood is sampled manually from the artery or vein which has various drawbacks. Recently a novel compact Time over Threshold (ToT) based Pr:LuAG-APD animal PET tomograph is developed in our laboratory which has 10% energy resolution, 4.2ns time resolution and 1.76mm spatial resolution. The measured value of spatial resolution shows much promise for imaging the blood vascular, i.e; artery of diameter 2.3-2.4mm, and hence, to measure PTAC for quantitative PET studies. To find the measurement time required to obtain reasonable counts for image reconstruction, the most important parameter is the sensitivity of the system. Usually small animal PET systems are characterized by using a point source in air. We used Electron Gamma Shower 5 (EGS5) code to simulate a point source at different positions inside the sensitive volume of tomograph and the axial and radial variations in the sensitivity are studied in air and phantom equivalent water cylinder. An average sensitivity difference of 34% in axial direction and 24.6% in radial direction is observed when point source is displaced inside water cylinder instead of air.**

I. Introduction

"A bloody future of clinical PET" was the title of editorial note by John Correia [1] for The Journal of Nuclear Medicine. Although quantitative positron emission tomography (PET) studies may be used in non-invasive monitoring of drug pharmacology [2], estimation of glucose consumption in human and the estimate of tissue fractional uptake through dynamic PET data analyzed with mathematical modelling of [^{18}F]florodeoxyglucose (^{18}FDG) kinetics [3]-[4] yet insertion of arterial lines, for the collection of blood samples, and processing for the measurement of activity are not compatible with the clinical PET. Various approaches like automated blood sampling and population based input functions are proposed to comfort the patients, reduce exposure to workers and efficient for medical centers but no one fulfils are the requirements [5]. We are developing an in-situ system which can provide blood time-activity curve (PTAC) without blood sampling and hence, avoiding the above mentioned drawbacks. We expect that this work will be helpful in developing an in-situ measurement system of radiotracer concentration in blood which will be able to solve the problems associated with conventional measurement system.

[1]Azhar H. Malik is PhD student of Department of the Nuclear Engineering and Management, University of Tokyo, 7-3-1 Hongo, Bunkyo, Tokyo 113-8656, Japan. e-mail: azhar2932@gmail.com

[2]Kenji Shimazoe is with the Department of Bio Engineering, University of Tokyo, 7-3-1 Hongo, Bunkyo, Tokyo 113-8656, Japan.

[3]Hiroyuki Takahashi is with the Department of Nuclear Engineering and Management, University of Tokyo, 7-3-1 Hongo, Bunkyo, Tokyo 113-8656, Japan.

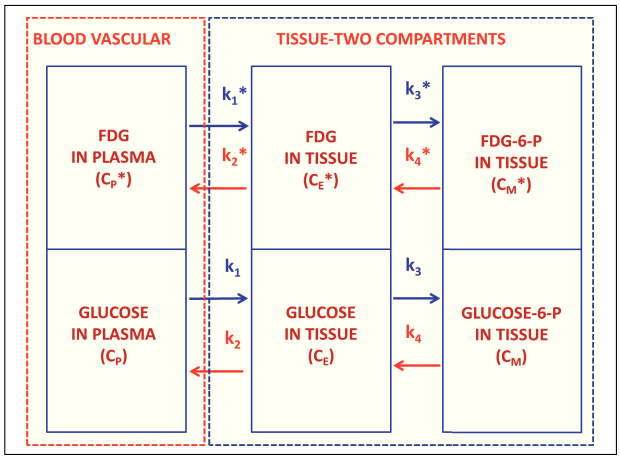

Fig. 1. Three compartmental model (vascular space, tissue space for FDG and glucose, and tissue space for $FDG-6-P$ and glucose-6-P) of FDG and glucose behaviour in brain. The asterisk is used to denote quantities associated with FDG or $FDG-6-P$ and those for glucose or glucose-6-P are without superscript. k_4^* = 0 for Sokoloff's model and is included in Huang's model.

A. Quantitative PET and three compartmental model

Dynamic acquisition together with kinetic modelling and blood sampling is the most accurate method of quantitative PET studies[6]. Among different mathematical models, three compartmental model is the most widely used model for describing the uptake and clearance of radioactive tracers in tissue [7]. This compartmental model was initially derived by Sokoloff et al. for [^{14}C]deoxyglucose (^{14}CDG) [8] and later extended by Huang et al. for ^{18}FDG [9]. The model is based on few assumptions and can be used to determine the rate constants and metabollic rate in tissue by using following equations,

$$C_i^*(t) = \frac{k_1^*}{\alpha_2-\alpha_1}[(k_3^*+k_4^*-\alpha_1)e^{-\alpha_1 t} + (\alpha_2-k_3^*-k_4^*)e^{-\alpha_2 t}] \otimes C_P^*(t). \quad (1)$$

$$R_i = C_P[C_i^*(T) - \frac{k_1^*}{\alpha_2-\alpha_1}[(k_4^*-\alpha_1)e^{-\alpha_1 t} + (\alpha_2 - k_4^*)e^{-\alpha_2 t}] \otimes C_P^*(t)].[(LC)\frac{k_2^*+k_3^*}{\alpha_2-\alpha_1} (e^{-\alpha_1 t} - e^{-\alpha_2 t}) \otimes C_P^*(t)]^{-1}. \quad (2)$$

In above equations, $C_i(t)^*$ is FDG concentration in tissue, $k_1^* - k_4^*$ are rate constants, α_1 and α_2 are combination of rate constants, $C_P(t)^*$ is FDG concentration in plasma, $C_P(t)$ is glucose concentration in plasma, and LC is lumped

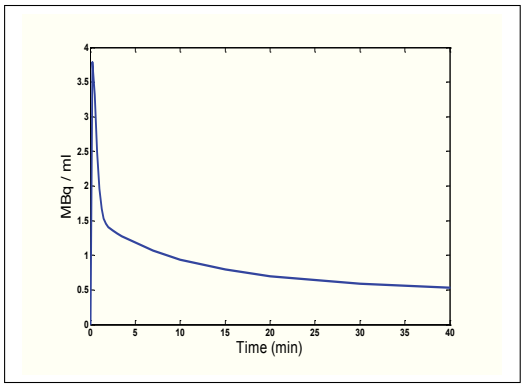

Fig. 2. Plasma time activity curve (PTAC) from relation obtained by fitting physical model to manually sampled blood activity data.

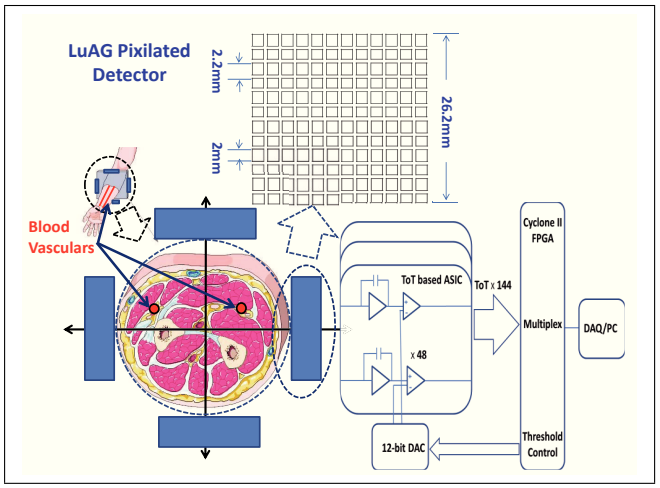

Fig. 3. Schematic diagram of measurement system.

constant [9]. The calculation of rate constants and metabolic rate requires: (1) the measurement of the total ^{18}F activity in local region of tissue at some appropriate time after FDG injection, (2) the plasma concentration of glucose, and (3) the plasma FDG concentration,or equally PTAC, from the time of injection to the time of measurement.

B. Plasma time activity curve

As explained in above section that PTAC is required for the quantitative PET studies. Using a physical model and curve fitting to measured blood sampled data, the PTAC may be obtained. The mathematical expression which explains activity in blood is given by the relation [4],

$$C_P^*(t) = (A_1 t - A_2 - A_3)e^{-\lambda_1 t} + A_2)e^{-\lambda_2 t} + A_3)e^{-\lambda_3 t}. \quad (3)$$

In (3), A's and λ's are model constants. Using above model, one such curve is given in Fig. 2. The activity reaches the maximum value shortly after injection, have fast and slow decay components and then almost constant after $15-20min$ of injection , see [4] for detail.

II. Compact pixelated LuAG-APD gamma-ray detector module

$Lu_3Al_5O_{12}$:Pr (LuAG:Pr) has attracted attention because of Pr^{3+}5d-4f emission at $310nm$ wavelength, non-hydroscopic nature, high density ($6.7g/cm^3$), high light output (around $20000photons/MeV$), very short decay time ($20ns$), and a good energy resolution (4.6% at $662keV$). Recently a novel compact Time over Threshold (ToT) [10] based Pr:LuAG-APD animal PET tomograph was developed in our laboratory with following characteristics, 8 block detectors, crystal to crystal detector ring size $72.5mm$, radial Field Of View (FOV) $34.5mm$ and axial FOV $25mm$ [11]. Fig. 3 shows the schematic diagram of four detector blocks system, forearm cross-section along with highlighted ulnar and radial arteries (sources to be imaged to measure activity) as well as one pixelated block detector and front-end electronics. Each detector block consists of 12×12 arrays of $2 \times 2 \times 10mm^3$ crystals coupled with 12×12 UV-enhanced avalanche photo diode (APD) arrays for individual readout [11]. Our developed PET tomograph has 10% energy resolution, $4.2ns$ time resolution and $1.76mm$ spatial resolution which shows much promise for blood vascular activity measurements [11]. In first experiment a columnar ^{22}Na source is imaged and $1.76mm$ spatial resolution, without subtracting the source dimension contribution in full width half maxima (FWHM), is obtained. The spatial resolution of the system shows much promise to image the blood vascular having diameter in the range $2.3 - 2.4mm$. Sensitivity and spatial resolution have prime importance in calculation of measurement time to obtain reasonable counts for image reconstruction and blood vascular image formation. We present the Electron Gamma Showers 5 (EGS5) simulation results of four block detectors LuAG-APD PET tomograph with the expectation that this work will be helpful in developing an in-situ measurement system of radiotracer concentration in blood which may comfort the patients, reduce exposure to workers and efficient for medical centers.

III. Monte Carlo EGS 5 code and simulation model

EGS5, alongwith other codes like Monte Carlo N-Particle Transport Code (MCNP), GEometry ANd Tracking (GEANT4), is an important radiation-matter interaction simulation tool widely used for simulation of many problems of high energy physics. It is used as reference model for the following Monte Carlo codes performing the studies of electromagnetic showers [12]. In case of compact LuAG-APD system, four block modules, each with 144 pixels, at 90^o were considered. A point source at center of gantry (COG) was assumed to be emitting the positron which annihilates to two $511keV$ oppositely moving gamma rays. These gamma rays are detected as coincident count if they simultaneously deposit energy greater than or equal to lower level of energy window (LLW). The coincident counts were used to find the sensitivity of system in units of cps/kBq which was used to determine the measurement time required to obtain reasonable counts for image reconstruction.

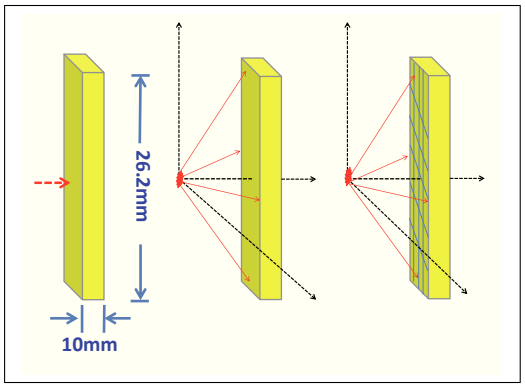

Fig. 4. (Left) Parallel beam of gamma rays incident on the center of LuAG slab detector $26.2 \times 26.2mm^2$ (Middle) Point source at $10cm$ from same LuAG slab detector (Right) Point source at $10cm$ and the slab detector is segmented into 144 pixels of size $2 \times 2mm^2$ with air gap of $0.2mm$.

TABLE I

LuAG DETECTION PROPERTIES AND SEGMENTATION EFFECT

	Det. Effic. (%)	Compt. Scat. (%)	Full Ener. (%)	Photo Frac. (%)
Parallel beam on slab det.	50.8	16.2	34.6	68.2
Point Source and slab det.	44	16.9	27.1	61.5
Point Source Pixel. det.	49.6	35.1	14.6	29.4

IV. SIMULATION RESULTS AND DISCUSSIONS

A. LuAG-APD small animal PET system

1) Radiation detection properties of LuAG: A typical small animal PET scanner consists of many rings of detector modules made of scintillating crystals of radial thickness. The detection properties of LuAG for different cases, shown in Fig. 4, are summarized in Table I. Using the previously reported values of attenuation coefficient($\mu = 0.106cm^2/g$), density ($\rho = 6.7g/cm^3$)[13] and thickness of $1cm$, we found the theoretical value of interaction probability as 50.8% whereas, EGS5 simulation value was found to be 50.81% with difference of 0.08%. Finally the slab is segmented, as shown in Fig. 4, and it was found that the value of photofraction reduces drastically from 61.5% to 29.4% when we segment the slab detector into pixels.

2) Sensitivity of LuAG-APD animal PET system: Spatial resolution as well as sensitivity are two important parameters to image a source, blood vascular in this case, while separating it clearly from neighbouring sources, nerves and muscles, and obtaining the reasonable counts for image reconstruction with shortest measurement time interval. Our main focus in this paper is on the variation of the sensitivity in axial and radial direction as well as the difference in sensitivities values in air and water. In small animal three dimension (3D) PET systems, the sensitivity is not uniform throughout the sensitive volume. Thus the knowledge of sensitivity variation is very important to measure the activity of selected region of interest. Usually, the maximum sensitivity is at COG and in the axial direction, the variation in sensitivity is off triangular shape [14]. Also the sensitivity depends on the selection of energy window which is very important to register only the true coincident counts and reject the scattered ones. In our simulations, we selected the LLW and if deposited energy was greater or equal to LLW, it was counted under full energy peak. For three LLW values of $200keV$, $250keV$ and $300keV$, the sensitivity values at COG of tomograph are shown in Table II. For LLW lower than $340keV$ some part of Compton continuum is included under full energy peak. It increases sensitivity if it is scattered from the pixel but distort image if scattered inside the phantom equivalent cylinder and deposited energy in the pixel which is greater than or equal to LLW. Further study is needed to account for the compromise to increase the sensitivity at cost of the degradation in spatial resolution along with the proper scattering corrections. We studied the axial variation of sensitivity with four LuAG-APD block detectors in which only opposite blocks of detectors were joined to detect coincident counts.

3) Sensitivity with phantom equivalent cylinder: For the most of the newly developed detectors, initial measurements are done with point source [11]. The medium is normally air and point source is moved through it, but as artery is inside forarm and phantoms are used which contain material equivalent to water for flesh, muscles and blood [15]. Thus, we used a $5cm$ cylinder to approximate the forarm phantom in our simulations and the sensitivity variation in axial direction is studied and the simulation results are shown in Fig. 5. It is clear that the sensitivity is nearly 60% of that in air at COG when point source is inside the cylinder containing water. The difference decreases as we move away from center. The variation in difference in shown in Fig. 6 and the average difference is 34%. Similarly average difference in radial direction was found to be 24.6%. The important conclusion from above results is that the characterization of system is normally done with air as medium between source and detector modules and as the sensitivity of system is reduced in case of phantom so we should consider the effect in case of actual measurements. The difference is quite high and we should calculate measurement time by considering the sensitivity value with water cylinder.

4) Spatial Resolution: Spatial resolution, expressed as FWHM, is the ability of a system to separately detect the features of object to be imaged. In present case, the artery is inside the arm and we want to clearly detect it to measure the activity in blood. Our goal is to image the artery in 3D and calculate its volume and hence finally the volumetric activity in blood from the image by selecting the area of interest.The pixel size is $2mm$ and the intrinsic resolution is 1mm. The results of first experiment, $1.76mm$ FWHM and

TABLE II

SENSITIVITY(cps/kBq) AT CENTER FOR POINT SOURCE.

LLW (keV)	2 Block Detectors	4 Block Detectors
250	0.99	1.98
300	0.64	1.27
350	0.42	0.83

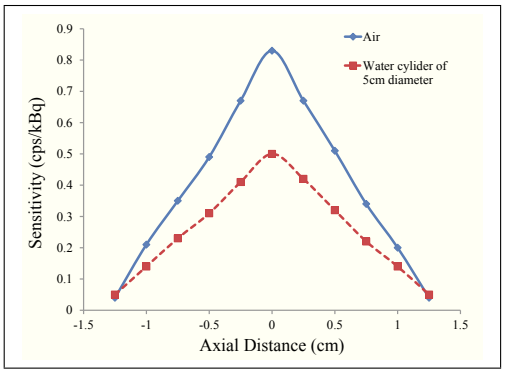

Fig. 5. Comparison of sensitivity variation with axial displacement of point source in air and inside phantom equivalent water containing cylinder.

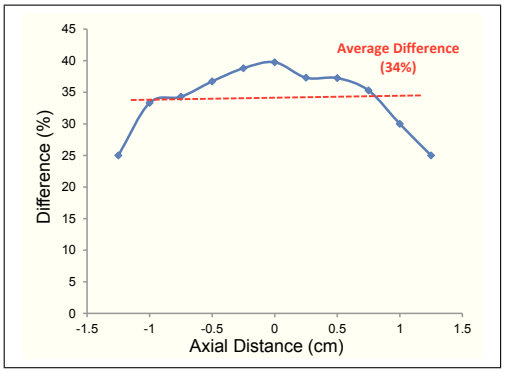

Fig. 6. Difference(%) in sensitivity in air and that in water with axial distance. The cylinder has $5cm$ diameter with point source along its axis.

$3.20mm$ FWTM, when using columnar ^{22}Na source[11], are very encouraging to use the system for imaging blood vascular.

5) Measurement Time: The measurement time is an important parameter to be considered for clinical applications of small animal PET system to measure radiotracer concentration in blood. The study of sensitivity variation and determination of its numerical value may be very helpful in this regard. Considering $350keV$ LLW and only oppositely joined four detector blocks PET tomograph having sensitivity value of $0.83cps/kBq$, we can collect 70,000 coincident counts for image reconstruction in $17.5min$ in air and $29.2min$ in phantom after $20min$ of injection. If we double the blocks of tomograph, the measurement time may be reduced to $8.8min$ and $14.6min$. Finally we constructed a cylindrical source from point sources at different positions to guess the sensitivity for blood vascular which comes out to be $0.25cps/kBq$ inside the phantom and thus measurement time of $25min$ with 8 block tomograph. Reducing the crystal to crystal distance, joining more blocks to register coincident counts, increasing the crystal thickness, increasing number of rings may increase the sensitivity and hence reduce the measurement time.

V. Conclusions

In order to utilize the full potential of quantitative PET, we have to avoid the blood sampling. Newly developed compact LuAG-APD based animal PET tomograph shows much promise regarding the measurement of blood vascular activity, and hence radiotracer concentration in blood. The study shows that an average difference in sensitivities in air and that in water in axial and radial directions is quite high and we should consider this difference for the calculations of measurement time. The measurement time to obtain the reasonable counts for artery image reconstruction is still high and we are hopeful to reduce it through different options. The high spatial resolution, option to increase sensitivity through inclusion of more detector blocks, flexible arrangement and reasonable energy resolution makes LuAG-APD tomograph as the choice of further study.

References

[1] J. Correia, A bloody future of clinical PET, J. of Nucl. Med., vol. 33, pp. 620-622, 1992.
[2] R. Myers, The biological application of small animal PET imaging, Nucl. Med. Bio., vol. 28, pp. 585-593, 2001.
[3] A. Bertoldo, P. Vicini, G. Sambuceti, A. A. Lammertsman, O. Parodi, and C. Cobelli, Evaluation of compartmental and spectral analysis models of [^{18}F]FDG kinetics for heart and brain studies with PET, IEEE Trans. on Biomed. Engg., vol. 45, pp. 1429-1448, Dec. 1998.
[4] D. Feng, K. P. Wong, C. M. Wu, and W. C. Siu, A technique for extracting physiological parameters and the required input function simultaneously from PET image measurements: theory and simulation study, IEEE Trans. on Inform. Tech. in Biomed., vol. 1, pp. 243-254, 1997.
[5] S. Eberl, A.R. Anayat, R. R. Fulton, P. K. Hooper, and M. J. Fulham, Evaluation of two population based input functions for quantitative neurological FDG PET studies, Eur. J. Nucl. Med., vol. 24, pp. 299-304, March 1997.
[6] M. Bentourkia, Kinetic modeling of PET-FDG in the brain without blood sampling, Comp. Med. Imag. and Graph., vol. 30, pp. 447-451, 2006.
[7] P. E. Valk, D. L. Bailey, D. W. Townsend, and M. N. Maisey, Positron Emission Tomography: Basic Science and Clinical Practice. New York: London: Springer, 2003.
[8] L. Sokoloff, M. Reivich, C. Kennedy, M. H. D. Rosiers, C. S. Patlak, K. D. Pettigrew, O. Sakurada, and M. Shinohara, The [^{14}C]deoxyglucose method for the measurement of local cerebral glucose utilization: theory, procedure, and normal values in the conscious and anesthetized albino rat, J. of Neurochem., vol. 28, pp. 897-916, 1977.
[9] S. C. Huang, M.E. Phelps, E. J. Hoffman, K. Sideris, C. J. Selin, and D. E. Kuhl, The [^{14}C]deoxyglucose method for the measurement of local cerebral glucose utilization: theory, procedure, and normal values in the conscious and anesthetized albino rat, Am. J. Physiol., vol. 238, pp. E69-E82,1980.
[10] K. Shimazoe, Y. Wang, H. Takahashi, K. Kamada, M. Yoshino, J. Kataoka, Y. Yamaya, T. Yanagida, A. Yoshikawa, and K. Kumagai, Novel Front-end pulse processing scheme for PET system based on pulse width modulation and pulse train method, IEEE Trans. Nucl. Sci., vol. 57, pp. 782-786, April 2010.
[11] K. Shimazoe, H. Takahashi, B. Shi, T. Furumiya, J. Ooi, Y. Kumazawa, and H. Murayama, Time over threshold based digital animal PET (TODPET), in Conf. Rec. 2011 IEEE Nucl. Sci. Symp., MIC15.S-44, pp. 3267-3271.
[12] W. R. Nelson, and C. Field, Comparison of EGS5 simulations with experiment, Nucl. Instr. Meth. A, vol. 572, pp. 1083-1093, 2007.
[13] M. Conti, L. Eriksson, H. Rothfuss, and C. L. Melcher, Comparison of fast scintillators with TOF PET potential, IEEE Trans. Nucl. Sci., vol. 56, pp. 926-933, 2009.
[14] C. D. Domenico, A. Motta, G. Zavattini, A. D. Guerra, C. Damiani, V. Bettinardi, and M. C. Gilardi, Characterization of the Ferrara animal PET scanner, Nucl. Instr. Meth A, vol. 477, pp. 505-508, 2002.
[15] P. Ruegsegger, and W. A. Kalender, A phantom for standardization and quality control in peripheral bone measurements by PQCT and DXA, Phys. Med. Biol., vol. 38, pp. 1963-1970, 1993.